





## Research Article

# Enhancing Tire Condition Monitoring through Weightless Neural Networks Using MEMS-Based Vibration Signals

Siddhant Arora,<sup>1</sup> Sridharan Naveen Venkatesh ,<sup>2</sup> Vaithiyanathan Sugumaran ,<sup>3</sup>  
Anoop Prabhakaranpillai Sreelatha ,<sup>4</sup> and Vetri Selvi Mahamuni ,<sup>5</sup>

<sup>1</sup>School of Computer Science and Engineering (SCOPE), Vellore Institute of Technology, Chennai Campus, Vandalur Kelambakkam Road, Chennai 600127, India

<sup>2</sup>Division of Operation and Maintenance Engineering, Luleå University of Technology, Luleå, Sweden

<sup>3</sup>School of Mechanical Engineering (SMEC), Vellore Institute of Technology, Chennai Campus, Vandalur Kelambakkam Road, Chennai 600127, India

<sup>4</sup>Sustainable Mobility Automobile Research Technology (SMART) Center, Department of Electronics and Communication Engineering, Amrita Vishwa Vidyapeetham, Amritapuri, India

<sup>5</sup>Department of Project Management, Mettu University, P.O. Box: 318, Metu, Ethiopia

Correspondence should be addressed to Vetri Selvi Mahamuni; [vetriselvi.m@meu.edu.et](mailto:vetriselvi.m@meu.edu.et)

Received 29 January 2024; Revised 17 April 2024; Accepted 24 April 2024; Published 10 May 2024

Academic Editor: Xiao He

Copyright © 2024 Siddhant Arora et al. This is an open access article distributed under the Creative Commons Attribution License, which permits unrestricted use, distribution, and reproduction in any medium, provided the original work is properly cited.

Tire pressure monitoring system (TPMS) has a critical role in safeguarding vehicle safety by monitoring tire pressure levels. Keeping the accurate tire pressure is necessary for confirming comfortable driving and safety, and improving fuel consumption. Tire problems can result from various factors, such as road surface conditions, weather changes, and driving activities, emphasizing the importance of systematic tire checks. This study presents a novel method for tire condition monitoring using weightless neural networks (WNN), which mimic neural processes using random-access memory (RAM) components, supporting fast and precise training. Wilkes, Stonham, and Aleksander Recognition Device (WiSARD), a type of WNN, stands out for its capability in classification and pattern recognition, gaining from its ability to avoid repetitive training and residual formation. For vibration data acquisition from tires, cost-effective micro-electro-mechanical system (MEMS) sensors are employed, offering a more economical solution than piezoelectric sensors. This approach yields a variety of features, such as autoregressive moving average (ARMA), statistical and histogram features. The J48 decision tree algorithm plays a critical role in selecting essential features for classification, which are subsequently divided into training and testing sets, crucial for assessing the WiSARD classifier's efficacy. Hyperparameter optimization of the WNN leads to improved classification accuracy and shorter computation times. In practical tests, the WiSARD classifier, when optimally configured, achieved an impressive 97.92% accuracy with histogram features in only 0.008 seconds, showcasing the capability of WNN to enhance tire technology and the accuracy and efficiency of tire monitoring and maintenance.

## 1. Introduction

Networks and technologies related to transport play a critical role in the economy by enabling the flow of goods across international borders by removing barriers for effective point-to-point travel and expediting the construction of infrastructure that raises the standard of living. This mobility depends on a vehicle's ability to travel great distances that

has been augmented through the invention of pneumatic tires which are considered as a significant advancement in this regard [1]. Constant advancements in tire design, weight reduction, and production methods enhance the economic possibilities for the tire sector. Finding the ideal balance between fuel economy, ride comfort, and occupant safety is a common concern shared by both designers and purchasers. Tires must be built with strength since they are

crucial safety components and must withstand challenging driving conditions [2]. Maintaining passenger safety, fuel efficiency, and utility requires proper tire care. While tires are made to endure for a very long period before replacement, things like inadequate inflation and reckless driving can limit their lifespan and cause quick wear, lower lifespan, and greater fuel consumption owing to increased rolling resistance [3]. This domino effect has long-lasting implications such as increased environmental impact from frequent refueling and early tire set disposal, as tire materials and additives are nonbiodegradable. The significance of prolonging tire lifespan is highlighted by this trifecta of problems which also include rising fuel prices, consumer desire for quality, and demand for cost-effectiveness [4]. A solution for both preventive and predictive maintenance is offered by tire condition monitoring systems (TCMS), which tracks tire pressure. There are two main types of TCMS that are described as follows:

- (i) In the case of direct TCMS, specific pressure sensors are located on tire valve stems or wheel hubs to send pressure information to the vehicle control unit.
- (ii) Indirect TPMS relies on the vehicle's existing sensors and employs advanced spectral analysis to infer tire pressure. These TPMS systems are crucial tools for improving safety, maximizing tire performance, and reducing environmental impact.

The field of TCMS has experienced substantial advances because of studies that focused at improving system operation and design. Recent research has provided insightful information building on the ground-breaking work of Hasan et al., which included pressure sensors, signal conditioning, radio frequency transmitters, and batteries [5]. Silalahi et al. built a TCMS incorporating pressure sensors, microcontrollers, and bluetooth connectivity [6]. For vehicle suspension, Lee et al. investigated an indirect TCMS employing adaptive extended Kalman filtering [7]. There are numerous fault diagnosis techniques each having their own advantages and disadvantages. As the complexity of features grows, traditional machine learning mandates explicit feature selection and extraction, posing a challenge. Rather than requiring explicit feature extraction, DNN algorithms enable direct learning from unprocessed data, such as image-based data plots. The extraction of raw input data from experimental setups is made easier by sensors and computers that have been specially outfitted. Among these techniques, vibration analysis stands out as being essential for identifying flaws. Signals from machine vibrations provide valuable information on the state of the machine. Anomalies that a visual inspection may have missed, such as imbalances, misalignments, and mechanical wear, can be discovered by evaluating these signals. Vibration analysis provides insights into component dynamics making it possible to identify issues early on before they worsen. Furthermore, it offers ongoing, unobtrusive monitoring without interfering with corporate operations. Although useful, vibration analysis has a few shortcomings. The utilization of specialized equipment, complex vibration pattern interpretation, and baseline data may be required for effective

analysis. In this research environment, vibration analysis becomes important for problem identification and tire condition monitoring, leveraging inherently present vibration signal information for accurate assessment and improved safety.

Deep neural networks (DNNs) are a type of artificial neural network that use layered design to gradually recognize complicated patterns in incoming data. In contrast to conventional machine learning, DNNs learn complex characteristics hierarchically over several layers, enabling input data to pass through various levels of processing. For problem detection and condition monitoring, this "deep" design has the potential to be disruptive and outperform current practices. Despite the early limitations of DNN applications in fault diagnosis, current developments have brought to light their importance. Various mechanical system conditions have been identified using DNNs. A deep statistical feature learning method for diagnosing the status of bearings and gearboxes was presented by Li et al. that makes use of characteristics from the frequency, time, and time-frequency domains [8]. Eighteen-time domain characteristics were used by Shao et al. to optimize deep belief networks for roller-bearing defect detection [9]. To diagnose the gearbox condition, Chen et al. suggested a convolutional neural network (CNN) that extracts information from the time and frequency domains. These instances show how DNNs have transformed from commonplace substitutes to essential instruments for quick fault state categorization [10]. Significant progress has been made in the field of fault diagnosis as a consequence of the use of machine learning (ML) and deep learning (DL). These technologies are appropriate for complicated condition monitoring scenarios since they offer automatic fault identification and categorization in brief time intervals. The confluence of ML and DL approaches with fault detection in recent years has opened the door for improved accuracy, efficiency, and dependability in locating and fixing mechanical system problems [11–13].

Weightless neural networks (WNNs) have emerged as a game-changing answer to the challenges of merging neural network techniques with low-power hardware devices, which are usually constrained by memory, power, and performance restrictions [14]. Bledsoe and Browning introduced WNNs in 1959, which was a significant development in hardware-optimized neural network approaches. WNNs, also known as n-tuple classifiers, offer certain benefits that set them apart:

- (i) Effective hardware integration: WNNs are designed to readily integrate into hardware environments with constrained resources for low-power devices [15].
- (ii) Swift and simplicity of implementation: When hardware resources are limited, WNNs are preferable since they are much simpler to build than more complicated neural network architecture.
- (iii) Single iteration learning: WNN holds the capacity to learn from data in a single iteration; providing quick training and testing procedures is one of its most notable advantages.

- (iv) N-Tuple classifiers: Also known as n-tuple classifiers, WNNs represent a distinctive classification methodology that enhances their effectiveness and flexibility [16].
- (v) Improved training and testing speed: WNNs perform training and testing operations with astounding efficiency, meeting the needs of real-time or time-sensitive applications.
- (vi) Memory storage optimization: WNNs store knowledge in random-access memory (RAM), as opposed to the traditional strategy of storing information in network weights, as seen in normal multilayer feed-forward neural networks (MLFFNN). This results in optimized memory consumption [17].

However, despite the prospective benefits of WNNs, there are still several research gaps that need to be addressed for investigation and advancement:

- (i) Application Complexity: Although WNNs excel at integrating with hardware, further study is required to examine their adaptability and performance across a larger variety of complicated applications.
- (ii) Techniques for Optimization: Researching cutting-edge methods to improve the effectiveness and optimization of WNNs, particularly in terms of memory usage and power consumption, continue to be a major focus.
- (iii) Generalization Capability: Exploring the generalization capacities of WNNs in various data settings and their resilience to noisy or inconsistent input data is a crucial research direction.
- (iv) Real-World Deployment: To ensure WNNs' smooth integration and performance in real-time applications, research efforts should concentrate on their practical deployment in real-world systems.

### 1.1. Technical Contributions

- (1) The study includes a comprehensive analysis that covers four different fault scenarios: high, normal, puncture, and idle.
- (2) Vibration data were acquired from the pneumatic tire under varying conditions, ensuring precise measurements by affixing two 20 g weights to the tire. The data collection process was carried out using an economical MEMS accelerometer.
- (3) These recorded vibration signals were transformed to get statistical, histogram, and ARMA features. Moreover, the J48 decision tree algorithm was employed for the identification of prominent features.
- (4) Wilkes, Stonham and Aleksander Recognition Device (WiSARD), a weightless neural network classifier, was used to accurately classify the various events after the feature selection phase [18, 19].

- (5) The performance and accuracy of the classifiers were carefully examined by a methodical examination of numerous hyperparameters. Variables including bleach confidence, tic number, map type, bleach step, bit number, and bleach flag were systematically adjusted to evaluate their influence on classification results.
- (6) Comparing the results from various hyperparameters provided an important insight into the best features for monitoring tire condition, offering useful advice for practical application and improvement in TCMS.

*1.2. Novelty.* The application of the ground-breaking weightless neural network WiSARD classifier for the analysis of tire condition monitoring system is what makes this study special in terms of originality. This innovative approach relies on the affordable MEMS accelerometer sensor's ability to collect vibration signals which are then skillfully transformed into a variety of statistical, histogram, and ARMA features. Feature selection is meticulously carried out using the J48 decision tree approach to discover important traits. The next critical step in enhancing the efficacy of the methodology is to train the WiSARD classifier using these enhanced characteristics. The classifier accuracy is further improved by thorough hyperparameter tuning, yielding findings that are decisive. Notably, the study highlights the WiSARD classifier's outstanding capability in precisely identifying and diagnosing different characteristics, demonstrating its adaptability for numerous applications, and reaffirming its reputation as a game-changing innovation in the field of tire condition monitoring systems.

## 2. Experimental Studies

In this section, a comprehensive explanation of the experimental setup and the methodology employed for tire condition monitoring using weightless neural networks is presented.

*2.1. Experimental Setup.* In this experimental setup, a Maruti Swift Dzire, which is a front-wheel drive car, was employed as the test vehicle. The primary goal of the study was to capture vertical vibration signals that were generated specifically by the air-filled pneumatic tire, with their origin at the rear left wheel axis. To accomplish this, a triaxial MEMS accelerometer with the model number MMA7361L was meticulously affixed to the rear left wheel hub. Furthermore, a waterproof sealant was applied to ensure the accelerometer's protection against external influences and maintain its integrity. The selected accelerometer possesses a sensitivity of 206 mV/g, a frequency range that extends from 1 to 400 Hz, and a resonance frequency of 6 kHz. Data acquisition from the accelerometer primarily focused on the Y-axis of the accelerometer data, thus enabling the capture of vertical vibrations. For a visual representation of the MEMS accelerometer employed for the collection of vibration data, please refer to Figure 1.

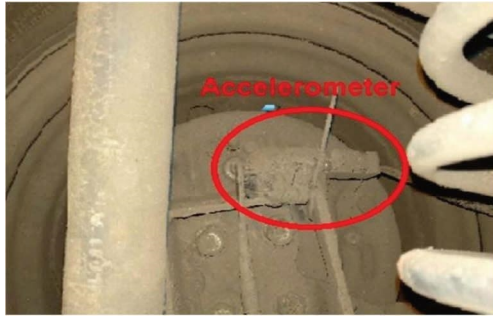


FIGURE 1: MEMS accelerometer mounted on the test vehicle rear axle.

**2.2. Method of Data Acquisition.** In this research, the NI USB-6001 DAQ device played a crucial role by converting analog signals into a digital format for further signal processing. The device's 12 input channels allowed simultaneous processing of multiple data streams from various sources, and its 14 bit resolution maintained data quality. With a maximum sampling rate of 20 kS/s, it enabled rapid data acquisition for real-time analysis. The integration of the NI USB-6001 DAQ device with the NI LabVIEW software ensured secure data transfer and efficient analysis, making it a vital component of the experimental setup, delivering accurate, high-quality data for subsequent analysis. Information from the accelerometer was conveyed to the DAQ through a shielded link, offering an additional safeguard against external electrical interference. Subsequently, the output from the DAQ was securely linked to the monitored computer system using NI LabVIEW software, guaranteeing the secure transmission and analysis of data.

**2.3. Experimental Procedure.** The data acquired for the study was derived from the vehicle in real-time running conditions on a national highway of India. The road conditions were nominally smooth, and the operating speed of the vehicle was restricted between 10 km/h and 100 km/h to simulate normal driving conditions. When assessing vibration signals, the following standards were adhered to.

- (i) **Sampling Frequency:** Vibration signal data were collected for tire rotation speeds between 10 kmph and 100 kmph. The maximum signal frequency obtained from the accelerometer for the 165/80 radial pneumatic tire utilized in this study was approximately 14.73 Hz, while the minimum frequency was close to 1.47 Hz. The choice of a sampling rate of 1 kHz was made in accordance with the Nyquist Sampling theorem.
- (ii) **Sample Length:** To establish computational balance across the four tire conditions under investigation, an acceptable sample length of 5,000 data points was chosen.

The wheel practiced multiple preparations for this experiment. Firstly, 40 g weights were attached to the rim to achieve balance. Subsequently, the pneumatic tire on the wheel was inflated to a pressure of 31 psi, establishing the

standard condition known as “normal.” The “high” state and its corresponding vibrational signals were generated by further increasing the pressure to 40 psi. The “puncture” scenario was simulated by lowering the tire’s pressure from 40 psi to 19 psi. Signals acquired at speeds under 10 kmph were labeled as “idle” due to their low amplitude. A dataset of 240 signals was generated with 60 data points collected for each condition. According to the Nyquist sampling theorem, the sampling frequency for each sample, which had 5,000 data points, was set at 1 kHz. Figure 2 represents the acquired vibration signals for every tire condition.

### 3. Methodology

The fault diagnosis process for evaluating tire conditions within the TCMS comprises three distinct phases: feature extraction, subsequent feature selection using the J48 algorithm, and feature classification using the WiSARD classifier. Figure 3 depicts the overall methodology of WiSARD classifier-based monitoring of tire condition.

**3.1. Feature Extraction.** Feature extraction is a prime machine learning process that transforms raw vibration data into a set of useful features that are appropriate for modeling and analysis. The objective of adopting feature extraction is to reduce the dimensionality of the data whilst keeping the information intact. The present study utilizes the capability of statistical, histogram, and ARMA features to portray the information derived from vibration signals [20]. The description of the features extracted is provided as follows.

- (i) **Statistical feature extraction** is a fundamental process that converts raw data such as tire pressure fluctuations from TCMS into concise and informative metrics. These metrics, referred to as features, play a pivotal role in unveiling key insights into the underlying characteristics of the data. In essence, these statistical features play a transformative role by translating intricate tire pressure fluctuation data from TCMS into meaningful attributes that harbor crucial insights into tire performance. Through the extraction and meticulous analysis of these features, the TCMS can discern deviations from the expected tire behavior, facilitating timely interventions and thereby augmenting overall operational efficiency and safety. This approach contributes to proactive maintenance practices, ensuring optimal tire health and longevity [21]. Table 1 in the supplementary data sheet details the descriptive statistical features extracted.
- (ii) **Histogram feature extraction** involves dividing the spectrum of tire pressure fluctuations into discrete intervals, each representing a specific range of values. Within each interval, the frequency or count of tire pressure data points is methodically calculated, thus quantifying the inherent distribution of pressure levels and visually depicting the patterns. In the realm of tire condition monitoring systems (TCMS), the histogram outlining tire pressure

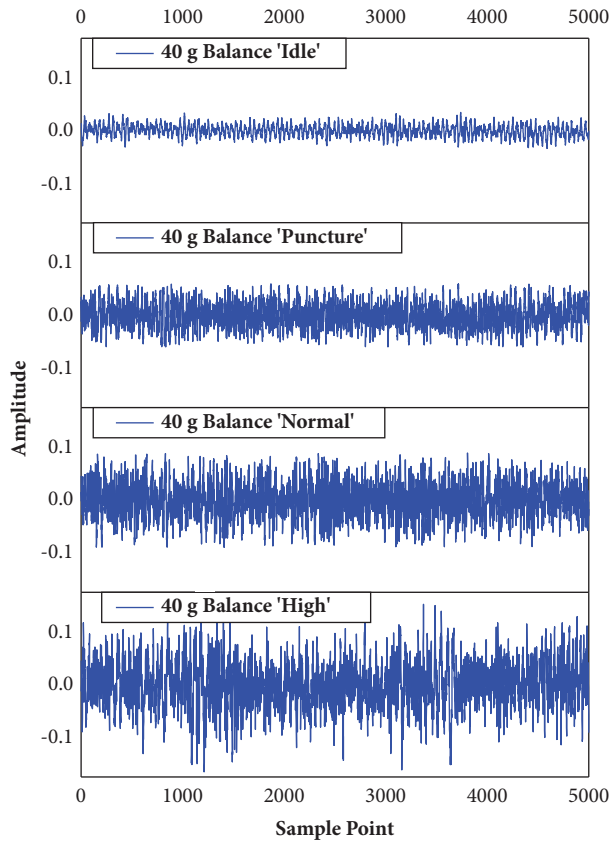


FIGURE 2: Vibration plots for every tire condition.

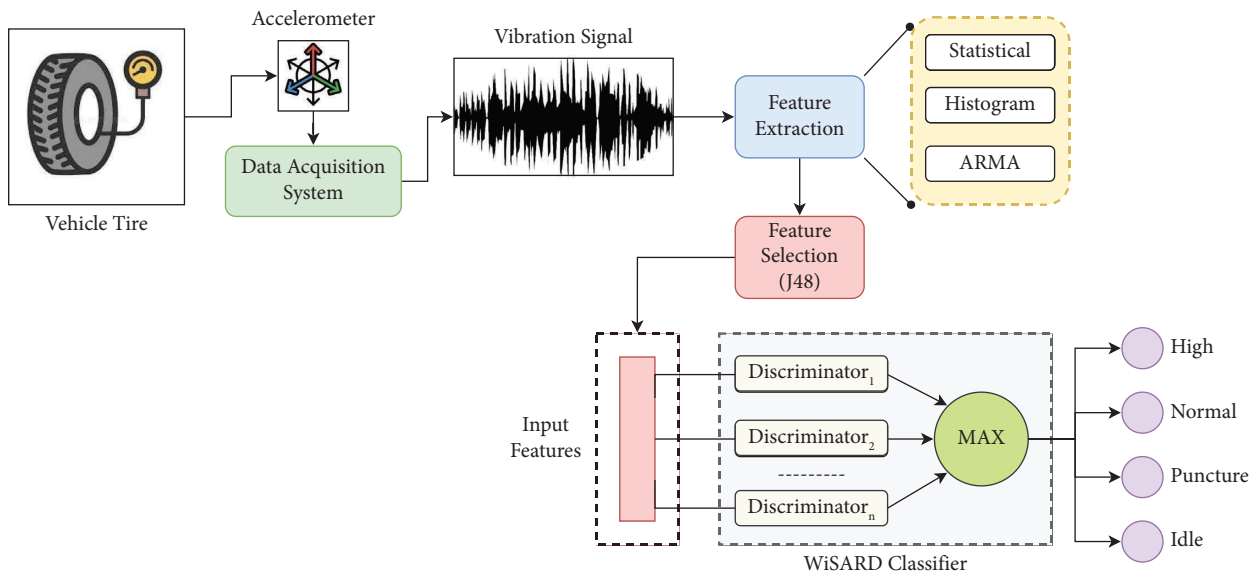


FIGURE 3: Overall methodology of WiSARD-based monitoring of tire condition.

amplitudes assumes significant importance [22]. During typical tire performance phases, the pressure fluctuations follow a distinctive pattern, translating into a characteristic form within the histogram. Typically, data points cluster around specific pressure ranges, vividly portraying the anticipated

operational behavior. In scenarios where anomalies like tire issues or irregularities emerge, disruptions within the pressure pattern become evident. Such deviations manifest as alterations in the amplitude distribution of the pressure signal. These deviations can result in shifts, unconventional peaks, or

troughs within the histogram, providing insights into potential tire condition irregularities. The structure of the histogram serves as a powerful tool for unearthing deviations from the standard distribution, enabling the detection of tire condition inconsistencies. This scrutiny of the histogram acts as a valuable mechanism to highlight deviations that may signify tire condition anomalies, prompting further in-depth analysis. In essence, histogram feature extraction not only quantifies pressure level distributions but also functions as a dynamic tool for identifying and investigating deviations in tire condition within the operational scope of TCMS. For the present study, 100 bins of histogram features were extracted and the most significant bin was selected using the J48 algorithm, as presented in Figure 4.

- (iii) Autoregressive moving average (ARMA) feature extraction represents an advanced technique for unraveling the intricate dynamics within time-series data, such as the tire pressure fluctuations observed in tire condition monitoring systems (TCMS). This method seamlessly combines two key elements—autoregressive (AR) and moving average (MA)—to unveil the underlying temporal dependencies shaping the evolution of the data over time. The autoregressive aspect, denoted as AR(p), deciphers the present signal value by considering its preceding p values, uncovering how past values contribute to the current state and encapsulating the data's memory and historical trends. Conversely, the moving average element, illustrated as MA(q), captures the impact of prior error terms on the current value, shedding light on the influence of past discrepancies on the trajectory of the pressure signal. In the realm of tire condition monitoring, these ARMA features hold paramount importance [23]. Deviations in the ARMA coefficients from established norms can serve as early indicators of tire anomalies or irregularities within the TCMS. The method's capability to capture cyclic patterns and variations in pressure signals deepens the comprehension of tire behavior, facilitating precise anomaly detection and thereby enhancing the overall effectiveness of tire performance monitoring and maintenance strategies. In the present study, ARMA orders were derived for a range starting from 2 to 30 and the optimum value was selected using the J48 algorithm, as shown in Figure 5.

**3.2. Feature Selection.** The presence of irrelevant or duplicate features in a dataset (due to unwanted noise) can induce a detrimental effect on the performance of machine learning models. Through careful selection of most significant features, the overall generalization capability of the model can be enhanced. Adopting useful features can aid in more consistent outcomes of the model that showcase minor overfitting with superior accuracy. An experimentation

using a relevant set of features can help in determining the impact of features on the final predictions [24]. This experimentation enables an informed decision-making through the selection of relevant features. The complete feature set can be streamlined to obtain faster model training and swift time for inference. Delimiting the occurrence of model overfitting is another prime advantage of feature selection. Overfitting in a model occurs due to the presence of a greater number of irrelevant features that can induce noise during training that can impose improper pattern learning. The model attention is focused around prominent information carriers present inside the data that can be represented through significant features. The study utilizes the feature selection capability of the J48 decision tree algorithm to detail the selected features in the form of an inverted tree shape. The feature of high importance is placed on the top while the features of less importance are placed in a descending manner. The less significant and non-contributing features are eliminated automatically through the rules formulated by the tree with the information gains. The selected features are presented in the branch and leaf nodes of the tree. The decision tree selected for statistical, histogram, and ARMA features is presented in Figures 6(a)–6(c), respectively.

### 3.3. WNN-Based Feature Classification (WiSARD Classifier).

Aleksander introduced an inventive digital neuron that employs RAM devices operating on Boolean logic. This concept laid the groundwork for the creation of weightless neural networks (WNNs), which utilize RAM-based neurons for their learning processes. Within this system, information is conveyed through truth tables stored in the RAM, constituting a vital element of WNN functionality [25]. Each WNN node specializes in recognizing a particular aspect of the input pattern, associated with a designated RAM address that formulates a mapping criterion. RAM network outputs are assigned with a value of 0 or 1. A distinguishing characteristic between weighted and weightless neural networks lies in their data processing strategies, wherein weightless neural networks utilize memory locations and hashing, while weighted neural networks allocate weights to an extensive array of features, as illustrated in Figure 7. This strategic choice affords WNNs a distinct edge in scenarios with limited memory resources, rendering them particularly appealing for real-world applications where optimizing memory overhead is essential. Figure 8 details the outline of RAM network [26].

Wilkes, Stonham and Aleksander Recognition Device (WiSARD), a pioneering innovation introduced by Aleksander and his collaborators, constitutes a notable stride in the realm of weightless artificial neural networks. This ground breaking n-tuple classifier presents a novel approach to pattern recognition, featuring a network of class discriminators, each equipped with a set of 'n' number of RAM nodes with 'n' number of address lines for intricate processing. At its core, the input retina orchestrates a pseudo-random mapping of  $N \times n$  bits, establishing input address lines across associated RAM nodes. The

TABLE 1: Descriptive statistical features extracted.

Statistical features	Description
Mean	The mean of the data is a representation of the data average value. It provides a center around which the data gather. Deviations from the norm might indicate abnormal behavior
Standard error	The standard error calculates the deviation between the sample mean and the actual population mean. It displays the mean precision
Median	The median serves as the middle point when data are sorted. It provides understanding of the data main topic and is robust to outliers
Mode	The mode is the value that is used the most. It can draw attention to persistent patterns in the data
Standard deviation	The standard deviation measures how far apart data points are in relation to the mean. The greater the value, the more variations are implied
Sample variance	Variance measures how far data points vary from the mean. It offers understanding of data variability
Kurtosis	Kurtosis is a feature of the distribution shape. High kurtosis points towards extreme values
Range	The range is the difference between the maximum and minimum values
Minimum	The minimum value signifies the lowest point of the data
Maximum	The maximum value represents the highest point of the data
Sum	The sum of all data points provides an insight into the overall magnitude
Skewness	Skewness indicates the distribution asymmetry. One side is favored when the skewness is high

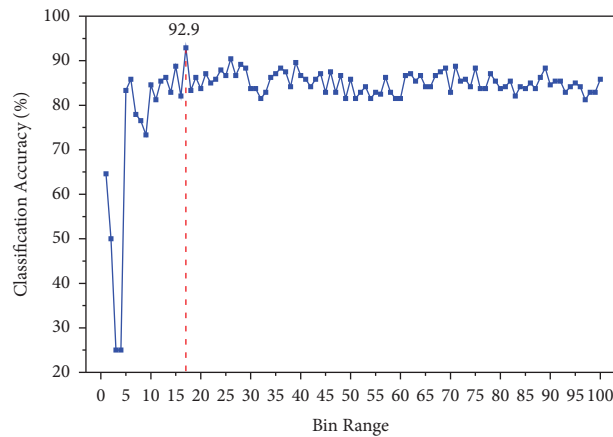


FIGURE 4: Bin selection for histogram features (bin 17).

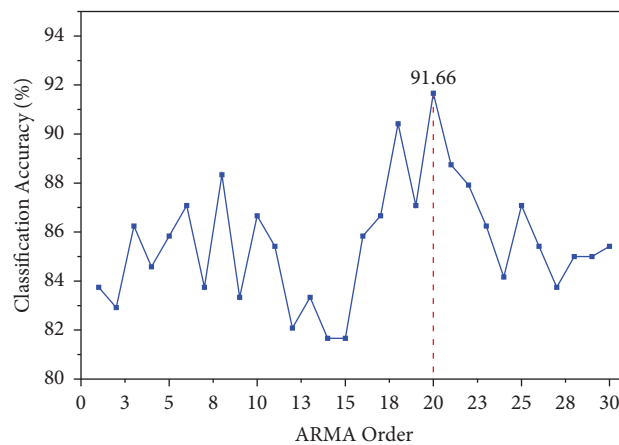
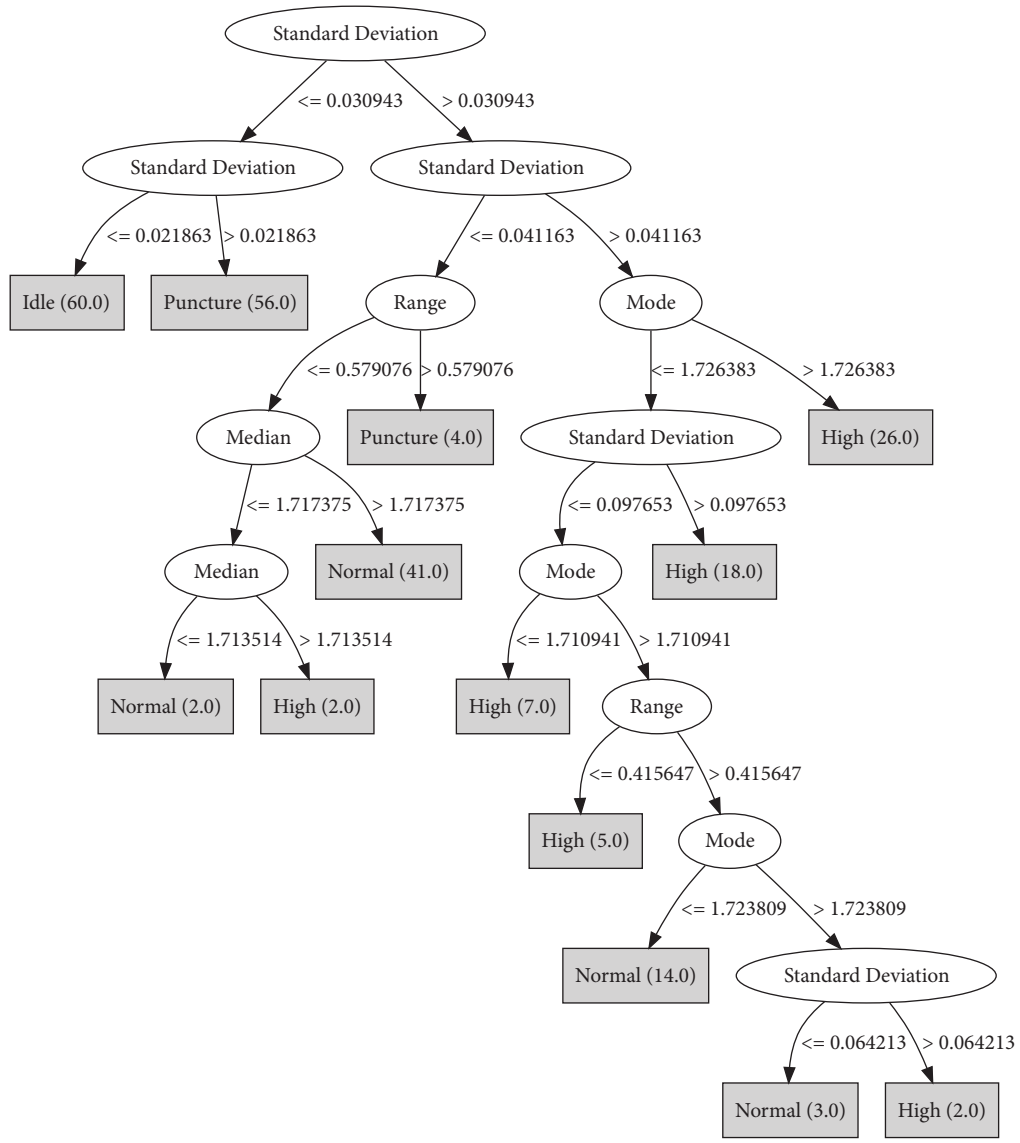


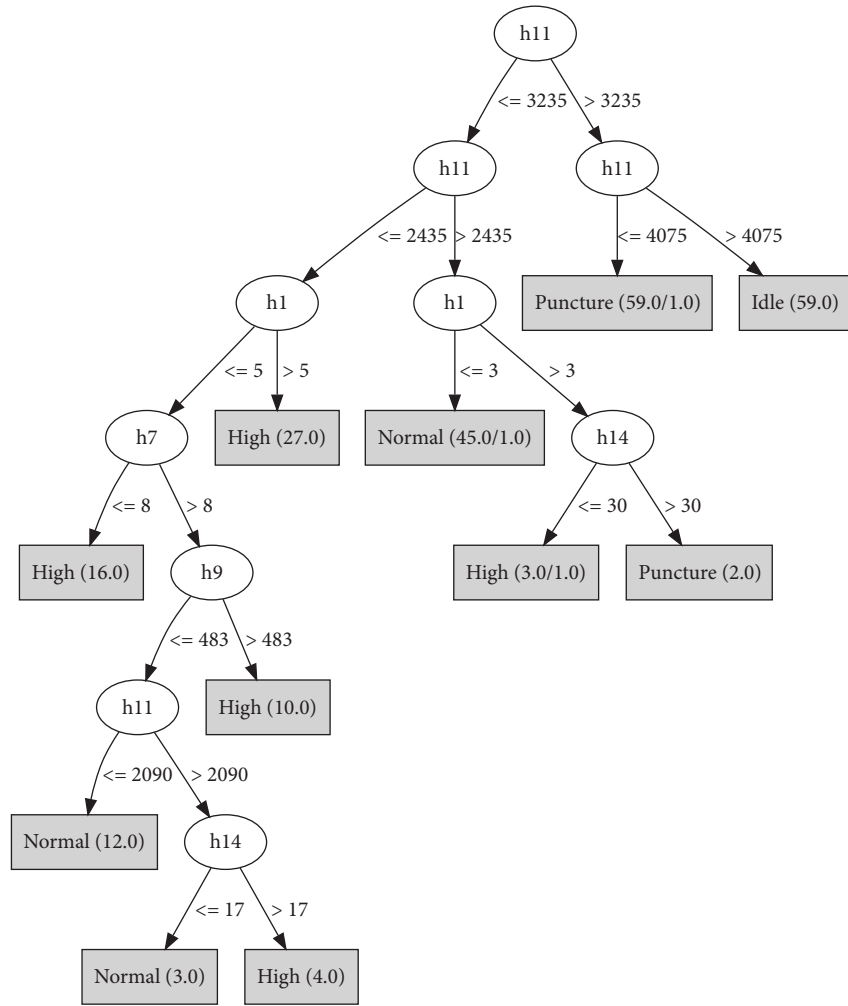
FIGURE 5: Order selection for ARMA features (order 20).



(a)

FIGURE 6: Continued.





(b)  
FIGURE 6: Continued.

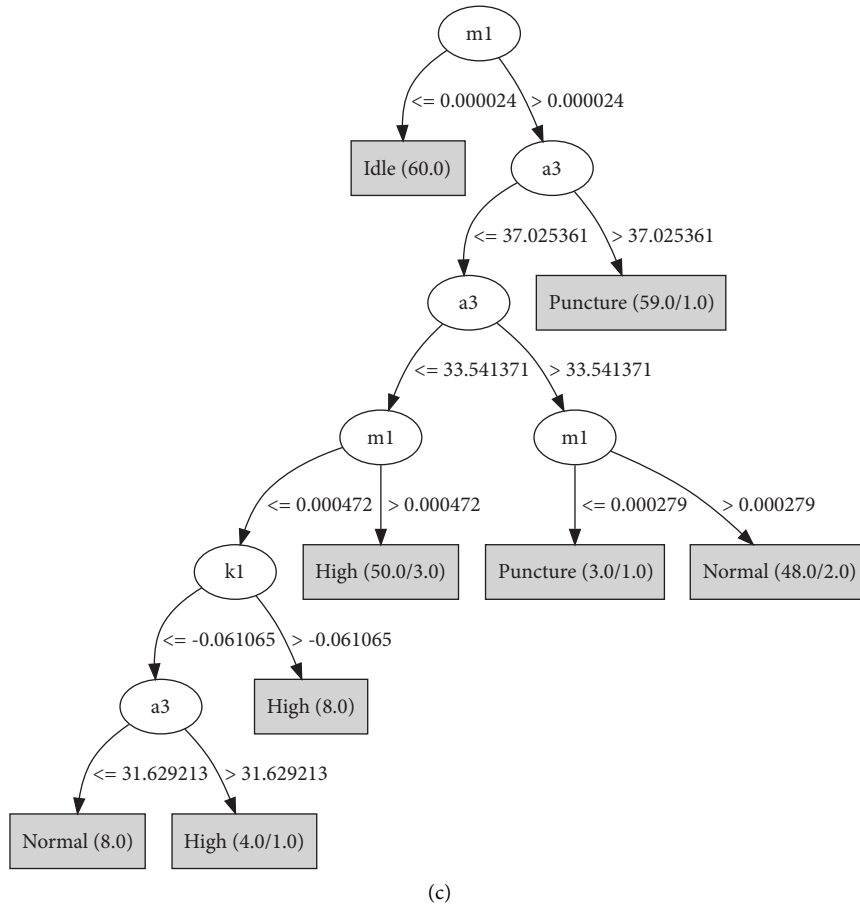


FIGURE 6: (a) Decision tree for statistical features. (b) Decision tree for histogram features. (c) Decision tree for ARMA features.

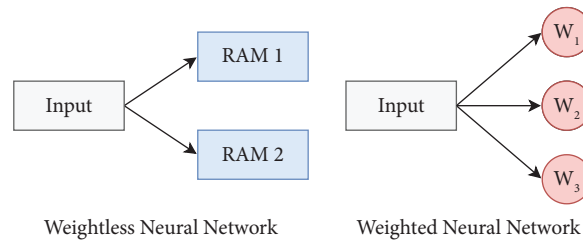


FIGURE 7: Basic difference in operation among weightless and weighted neural network.

architecture dynamism, dynamic address line allocation, and the inventive utilization of the input retina collectively position WiSARD as an exemplar of adaptable pattern recognition within artificial neural networks. Leveraging these benefits, WNN exemplified by WiSARD emerge as a preferred choice in contexts where computational efficiency, scalability, and real-time applicability are of paramount importance [27]. The overall workflow of steps involved in WiSARD classifier is presented in Figure 9 while the complete model of WiSARD classifier inbuilt with discriminator module is presented in Figure 10.

#### 4. Results and Discussion

The present study centers on assessing the performance of the WiSARD classifier in monitoring tire conditions. Four conditions of the tire, namely, puncture, high, idle, and normal were considered in the study. The WiSARD classifier performance relies on the numerous hyperparameters involved such as tic number, map type, bleach flag, bleach confidence, and bit number. For initial assessment, a training set with 80% of the initial data and a test set with 20% of the initial data were formulated. The experimentation was

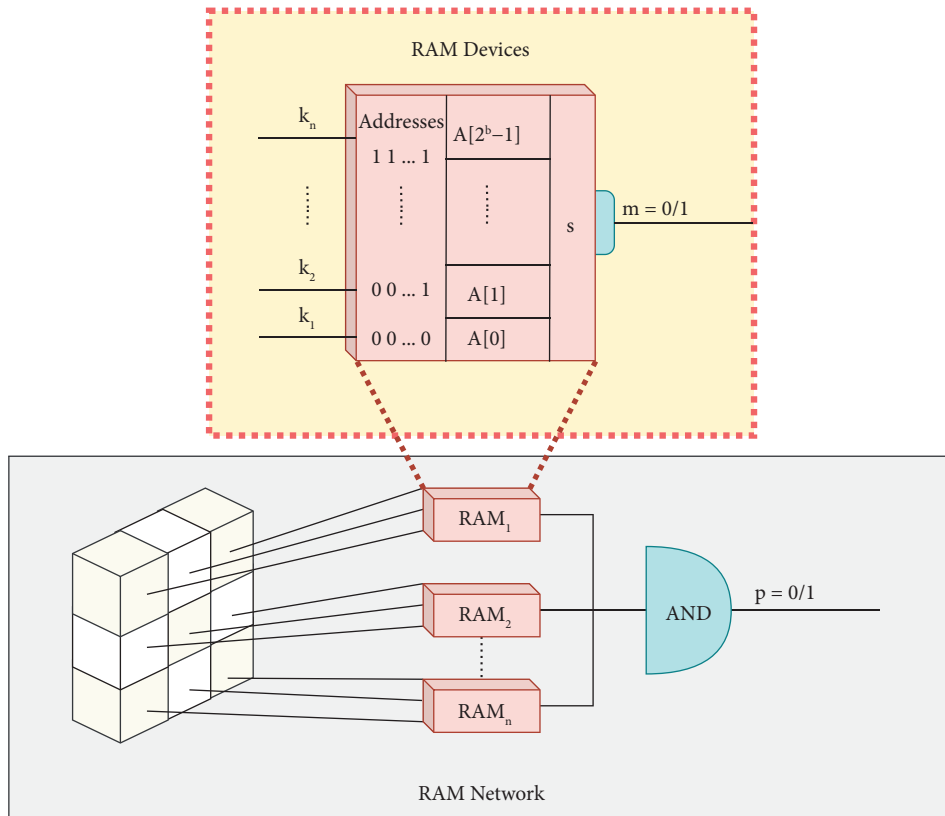


FIGURE 8: Outline of RAM devices in a RAM network.

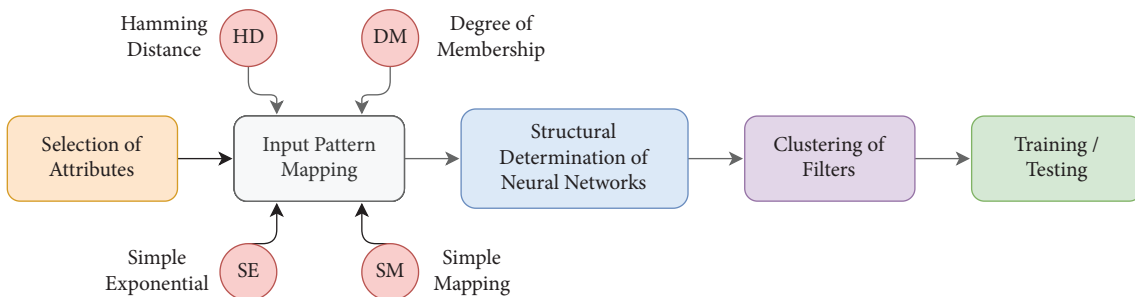


FIGURE 9: Overall workflow of the WiSARD classifier.

carried out to determine the optimal hyperparameter configuration of WiSARD classifier for every feature set to obtain superior performance.

**4.1. Effect of “Bit Number”.** The parameter “bit number” in the WiSARD classifier holds great importance, as it directly dictates the quantity of bits utilized in generating the sparse distributed representation (SDR). The choice of the number of bits has a substantial impact on both the classifier’s capacity and its precision. In the WiSARD classifier context, “bits” denote the specific binary units employed for demonstrating information. The classifier operates as a pattern recognition technique relying on a collection of randomly initialized binary bit cells for recognizing input patterns. To illustrate the consequences

of varying the bit number, Tables 2–4 offer a comprehensive overview of how this variation affects different accuracy measures. The optimal value, which consistently delivered the highest accuracy across these parameters, was carefully selected. This optimal value remained unchanged when adjustments were made to other hyperparameters. To ensure equitable experimental conditions, all parameters, apart from the bit number, were maintained at their default settings. Upon scrutinizing the outcomes presented in Table 4, a consistent pattern emerges: the utilization of a bit number set at 4 consistently resulted in higher accuracies compared to other bit number choices. Consequently, bit number 4 emerged as the favored and optimal selection, emphasizing its compatibility with improved accuracy across a range of evaluation metrics.

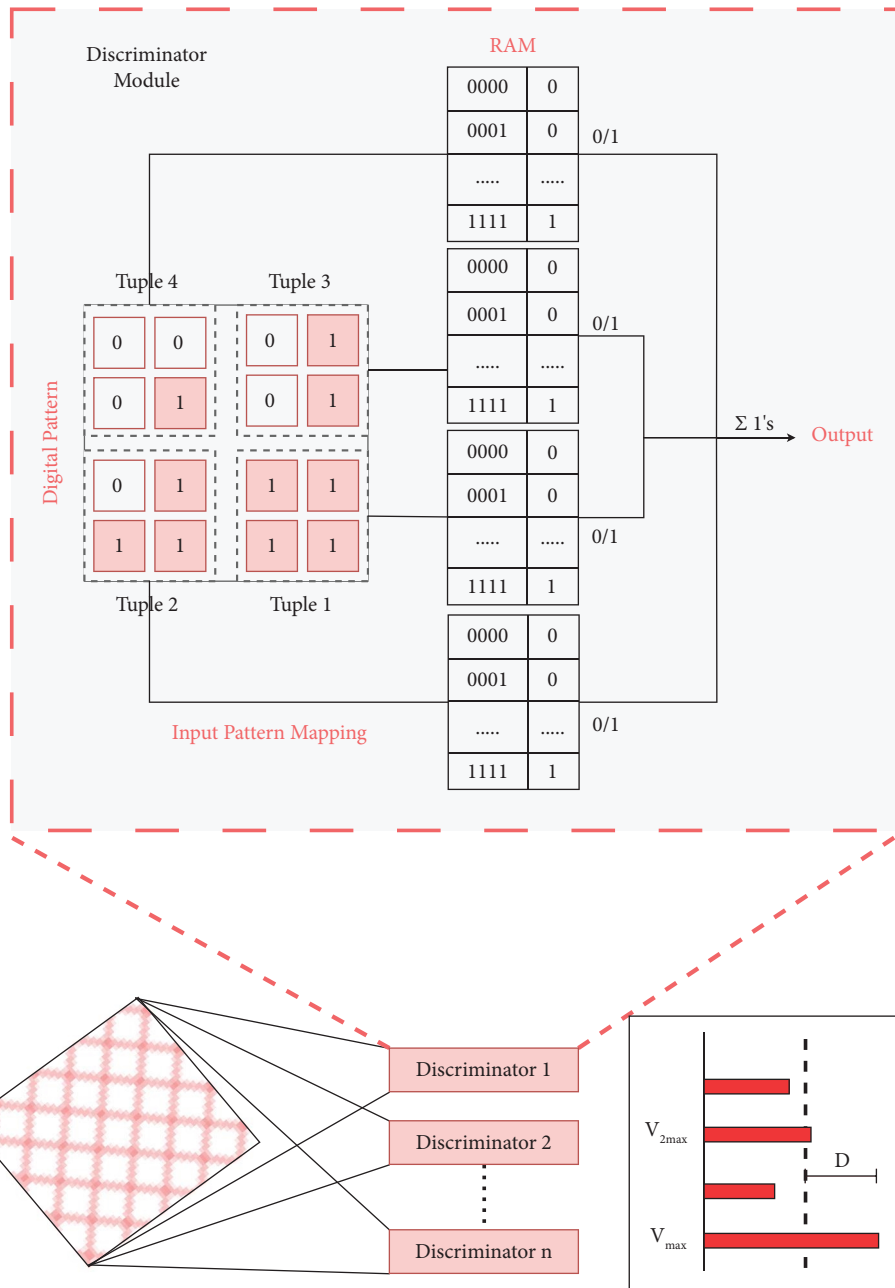


FIGURE 10: Complete model of the WiSARD classifier inbuilt with discriminator module.

TABLE 2: Training set accuracy for varying bit number.

Hyperparameter Bit No.	Statistical		Histogram		ARMA	
	Accuracy (%)	Times	Accuracy (%)	Times	Accuracy (%)	Times
4	98.54	0.058	93.23	0.078	98.75	0.096
8	99.79	0.040	95.63	0.044	99.79	0.070
16	100.00	0.054	97.92	0.054	100.00	0.060
32	100.00	0.044	98.44	0.038	100.00	0.060

4.2. *Effect of Bleach Confidence.* Within the WiSARD classifier, the adjustment of the prediction confidence is orchestrated by the bleach confidence parameter, contingent upon the likeness between incoming data and the

stored patterns. If the input pattern matches one of the stored patterns, the confidence level is increased; conversely, when there is no alignment, the confidence is reduced. This adaptation contributes to the enhancement

TABLE 3: Cross-validation accuracy for varying bit number.

Hyperparameter Bit No.	Statistical		Histogram		ARMA	
	Accuracy (%)	Times	Accuracy (%)	Times	Accuracy (%)	Times
4	86.45	0.022	89.27	0.018	92.60	0.024
8	88.02	0.010	89.37	0.016	93.43	0.014
16	89.89	0.012	88.74	0.014	94.27	0.012
32	90.20	0.014	90.52	0.014	94.06	0.010

TABLE 4: Test accuracy for varying bit number.

Hyperparameter Bit No.	Statistical		Histogram		ARMA	
	Accuracy (%)	Times	Accuracy (%)	Times	Accuracy (%)	Times
4	86.25	0.010	95.83	0.010	97.50	0.022
8	85.00	0.010	92.08	0.018	95.83	0.020
16	84.16	0.018	93.75	0.016	97.50	0.020
32	82.50	0.012	93.75	0.010	95.41	0.020

of the classifier’s predictive accuracy. The study has fine-tuned the bleach confidence values, and the outcomes are presented in Tables 5–7. The data in Table 7 reveal variations in validation accuracies, with training and testing accuracies staying consistent. Drawing from the presented findings, it can be deduced that the WiSARD classifier exhibited heightened accuracy levels for statistical, histogram, and ARMA features when the bleach confidence values were set to 0.70, 0.90, and 0.95.

**4.3. Effect of “Bleach Flag”.** The bleach flag in the WiSARD classifier operates as a binary indicator, determining the necessity for adjusting prediction confidence. If configured as “true,” it triggers the bleach confidence procedure, refining the confidence value. Conversely, when set to “false,” the confidence level remains unchanged. The bleach flag plays a vital role in governing when and how confidence adjustments take place within the classifier’s decision-making process. Given its binary nature, the bleach flag presents only two possible values: “true” or “false.” Tables 8–10 provide a visual representation of the collected outcomes concerning variations in the bleach flag.

**4.4. Effect of “Bleach Step”.** Within the domain of neural networks, the utilization of the bleaching process is aimed at mitigating overfitting, a situation wherein a model becomes overly specialized to the training dataset. Standard approaches to tackle overfitting encompass methods such as dropout, regularization, modifications to the model’s architecture, and early stopping. The control of the pace of the bleaching process is entrusted to the bleach step hyperparameter. A reduced value for the bleach step results in a more gradual bleaching process, whereas an increased value expedites it. Tables 11–13 provide an extensive examination of how the bleach step parameter influences performance metrics.

**4.5. Effect of “Map Type”.** The “map types” in the WiSARD classifier are associated with the methods used to link input patterns to the bit cells of the classifier, and this linkage directly impacts the performance of the classifier. Two utilized map types include linear and random.

- (i) Linear map: The linear map establishes a clear and consistently straightforward mapping structure. In the context of the linear map, input characteristics are methodically distributed and sequentially matched with specific bits within the bit cells. Each feature is distinctly linked to a particular bit, creating a direct one-to-one relationship from input to bits. For example, the first feature corresponds to the first bit, the next feature to the second bit, and this sequence remains consistent.
- (ii) Random map: Conversely, the random map entails dispersing input characteristics and associating them with bits in an irregular, nonsequential manner. This results in an unpredictable mapping from input to bit cells. Any feature can be paired with any bit without adherence to order, introducing a degree of variability and unpredictability into the mapping process.

The selection of the map type in the WiSARD classifier wields a significant influence over its performance and behavior. The linear map provides a systematic, predictable pattern that proves to be beneficial in scenarios where a distinct feature-to-bit relationship is desired. In contrast, the random map introduces an element of unpredictability, enhancing the classifier’s capacity to adapt to a wide array of data types and bolstering its generalization capabilities. The importance of choosing the suitable map type is underscored in Tables 14–16, highlighting its role in optimizing the classifier’s effectiveness. Essentially, map types determine the association between input characteristics and bits, and the decision between linear and random maps can be pivotal in achieving the intended classification results, with the former ensuring predictability and the latter offering adaptability.

TABLE 5: Training set accuracy for varying bleach confidence.

Hyperparameter Bleach confidence	Statistical		Histogram		ARMA	
	Accuracy (%)	Times	Accuracy (%)	Times	Accuracy (%)	Times
0.6	99.06	0.054	94.68	0.062	98.64	0.074
0.7	99.38	0.062	93.02	0.068	98.54	0.080
0.8	98.12	0.054	93.95	0.068	99.06	0.082
0.9	99.16	0.100	92.81	0.062	98.95	0.074
0.95	98.54	0.064	94.27	0.076	98.95	0.078

TABLE 6: Cross-validation accuracy for varying bleach confidence.

Hyperparameter Bleach confidence	Statistical		Histogram		ARMA	
	Accuracy (%)	Times	Accuracy (%)	Times	Accuracy (%)	Times
0.6	87.37	0.020	88.15	0.020	93.33	0.020
0.7	85.90	0.020	89.87	0.018	92.39	0.018
0.8	86.25	0.016	88.64	0.014	92.60	0.020
0.9	86.05	0.160	87.21	0.014	93.12	0.022
0.95	87.18	0.018	89.06	0.022	93.12	0.020

TABLE 7: Test set accuracy for varying bleach confidence.

Hyperparameter Bleach confidence	Statistical		Histogram		ARMA	
	Accuracy (%)	Times	Accuracy (%)	Times	Accuracy (%)	Times
0.6	85.83	0.026	94.58	0.010	96.25	0.02
0.7	87.08	0.010	95.00	0.022	97.50	0.022
0.8	86.66	0.010	94.49	0.014	96.66	0.020
0.9	85.41	0.014	95.83	0.014	94.58	0.020
0.95	85.83	0.022	95.41	0.026	97.08	0.020

TABLE 8: Training set accuracy for varying bleach flag.

Hyperparameter Bleach flag	Statistical		Histogram		ARMA	
	Accuracy (%)	Times	Accuracy (%)	Times	Accuracy (%)	Times
True	98.66	0.140	94.06	0.152	91.35	0.154
False	98.66	0.140	94.15	0.074	98.22	0.072

TABLE 9: Cross-validation accuracy for varying bleach flag.

Hyperparameter Bleach flag	Statistical		Histogram		ARMA	
	Accuracy (%)	Times	Accuracy (%)	Times	Accuracy (%)	Times
True	50.10	0.020	94.06	0.152	52.00	0.020
False	86.87	0.016	94.15	0.074	92.30	0.020

TABLE 10: Test set accuracy for varying bleach flag.

Hyperparameter Bleach flag	Statistical		Histogram		ARMA	
	Accuracy (%)	Times	Accuracy (%)	Times	Accuracy (%)	Times
True	86.66	0.026	95.41	0.036	88.33	0.030
False	86.25	0.024	95.83	0.010	96.66	0.020

4.6. *Effect of "Tic Number"*. The "tic number" within the WiSARD classifier is a critical parameter that dictates the number of bits assigned to each individual bit cell. This parameter wields significant influence over both memory capacity and the degree of precision in representing data. Opting for higher tic numbers enhances memory capacity,

enabling a more intricate and detailed data representation, which proves particularly beneficial for complex information. However, this choice necessitates a trade-off, as it leads to increased memory consumption and heightened computational complexity. Consequently, the selection of tic numbers entails a delicate equilibrium between memory

TABLE 11: Training set accuracy for varying bleach step.

Hyperparameter Bleach step	Statistical		Histogram		ARMA	
	Accuracy (%)	Times	Accuracy (%)	Times	Accuracy (%)	Times
1	98.83	0.124	93.83	0.086	98.54	0.086
2	98.22	0.136	93.14	0.060	98.86	0.074
5	98.86	0.120	94.06	0.052	98.85	0.070
10	97.82	0.106	94.18	0.038	98.86	0.076

TABLE 12: Cross validation accuracy for varying bleach step.

Hyperparameter Bleach step	Statistical		Histogram		ARMA	
	Accuracy (%)	Times	Accuracy (%)	Times	Accuracy (%)	Times
1	51.25	0.020	88.32	0.016	92.39	0.020
2	49.37	0.136	88.44	0.018	92.39	0.020
5	46.66	0.020	88.43	0.012	92.83	0.020
10	51.97	0.016	88.02	0.016	92.70	0.018

TABLE 13: Supplied test set accuracy for varying bleach step.

Hyperparameter Bleach step	Statistical		Histogram		ARMA	
	Accuracy (%)	Times	Accuracy (%)	Times	Accuracy (%)	Times
1	87.50	0.020	94.16	0.012	95.00	0.020
2	86.25	0.046	96.66	0.014	97.08	0.020
5	87.08	0.024	94.16	0.020	97.08	0.020
10	87.08	0.032	95.83	0.014	98.33	0.020

TABLE 14: Training set accuracy for varying map type.

Hyperparameter Map type	Statistical		Histogram		ARMA	
	Accuracy (%)	Times	Accuracy (%)	Times	Accuracy (%)	Times
Random	99.07	0.150	93.55	0.072	98.85	0.074
Linear	99.47	0.082	98.43	0.040	99.47	0.056

TABLE 15: Cross validation accuracy for varying map type.

Hyperparameter Map type	Statistical		Histogram		ARMA	
	Accuracy (%)	Times	Accuracy (%)	Times	Accuracy (%)	Times
Random	49.58	0.180	88.43	0.022	92.70	0.020
Linear	31.77	0.140	88.02	0.020	87.50	0.010

TABLE 16: Test set accuracy for varying map type.

Hyperparameter Map type	Statistical		Histogram		ARMA	
	Accuracy (%)	Times	Accuracy (%)	Times	Accuracy (%)	Times
Random	85.41	0.028	94.58	0.120	97.08	0.020
Linear	81.25	0.018	89.58	0.014	91.66	0.016

capacity and computational efficiency. Tables 17–19 furnish valuable insights into how diverse tic numbers impact the WiSARD classifier’s performance, providing informed guidance for varied application scenarios.

4.7. *Optimal Hyperparameter Selection.* Table 20 provides a visual representation of experiment outcomes, showcasing the selection of optimal hyperparameters as discussed in previous sections. The data presented in Table 20 emphasize

TABLE 17: Training set accuracy for varying tic number.

Hyperparameter Tic no	Statistical		Histogram		ARMA	
	Accuracy (%)	Times	Accuracy (%)	Times	Accuracy (%)	Times
1	26.56	0.001	43.75	0.001	26.56	0.001
10	61.14	0.006	81.87	0.002	83.02	0.002
20	81.56	0.0100	84.27	0.018	89.89	0.010
50	90.52	0.018	90.83	0.010	95.10	0.016
100	94.88	0.034	90.05	0.022	95.20	0.030
256	99.37	0.114	93.14	0.072	98.95	0.078

TABLE 18: Cross-validation accuracy for varying tic number.

Hyperparameter Tic no	Statistical		Histogram		ARMA	
	Accuracy (%)	Times	Accuracy (%)	Times	Accuracy (%)	Times
1	23.66	0.001	43.02	0.001	25.52	0.001
10	47.70	0.002	79.58	0.010	78.43	0.002
20	53.95	0.001	82.60	0.001	85.72	0.020
50	54.37	0.002	87.40	0.002	90.62	0.100
100	51.14	0.010	88.33	0.010	92.60	0.008
256	49.78	0.018	88.43	0.014	93.12	0.02

TABLE 19: Test set accuracy for varying tic number.

Hyperparameter Tic no	Statistical		Histogram		ARMA	
	Accuracy (%)	Times	Accuracy (%)	Times	Accuracy (%)	Times
1	27.08	0.001	33.33	0.022	22.91	0.010
10	56.66	0.020	95.83	0.001	82.49	0.001
20	74.99	0.003	95.41	0.003	82.50	0.002
50	78.75	0.006	97.92	0.008	90.83	0.004
100	81.66	0.010	97.08	0.010	93.75	0.010
256	85.83	0.020	96.24	0.016	96.66	0.020

TABLE 20: Optimal hyper parameters of WiSARD classifier.

Features	Bit number	Bleach confidence	Bleach flag	Bleach step	Map type	Tic number	Accuracy (%)	Time
Statistical	4	0.7	True	1.0	RANDOM	256	85.83	0.020
Histogram	4	0.9	False	10.0	RANDOM	50	97.92	0.008
ARMA	4	0.7	False	10.0	RANDOM	256	96.66	0.020

that, by utilizing histogram features, we achieved an impressive 97.92% classification accuracy. To evaluate the model's performance under these optimal hyperparameter settings, we employed a confusion matrix, as illustrated in Figure 11. A confusion matrix, an essential tool for assessing classification algorithms, provides a comprehensive overview of the algorithm's predictions on a test dataset, allowing for a detailed comparison between predicted and true labels. In this specific multiclass classification scenario, where distinguishing between faulty and nonfaulty tires is of utmost importance, the matrix exhibited a remarkable level of precision, with minimal misclassifications. It is worth underscoring that the model's testing time was exceptionally brief, measuring just 0.008 seconds, which implies its potential applicability in real-time fault diagnosis systems. The WiSARD classifier obtained accurate classification results

with a bit number of 4 and tic number of 50 for the histogram features. Furthermore, the research effectively demonstrates the proficiency of the proposed fault diagnosis approach employing the WiSARD classifier.

*4.8. Performance Comparison with State-of-the-Art Techniques.* The present section displays the superior performance of the proposed technique over various methodologies portrayed in a lot of literature. The classification accuracy obtained using the proposed methodology is compared with various works of literature carried out over the years as presented in Table 21. The presented table underscores the noteworthy success of the proposed approach, surpassing all preceding endeavors with a remarkable classification accuracy of 97.92% and a minimal



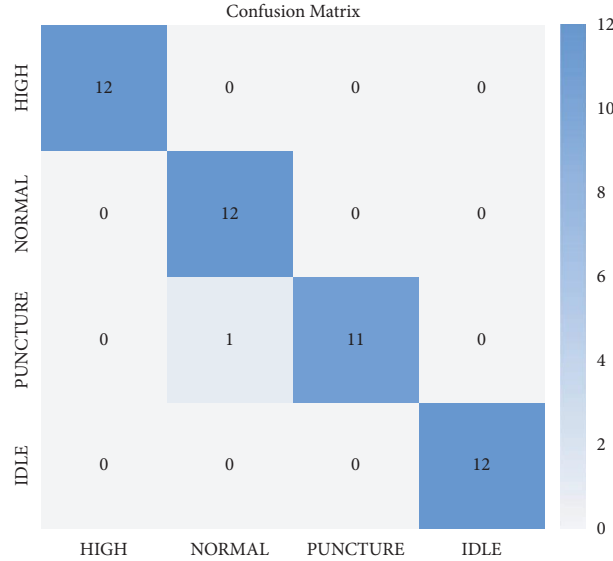


FIGURE 11: Confusion matrix of the WiSARD classifier for histogram features.

TABLE 21: Performance comparison with different approaches.

Ref no	Technique	Accuracy (%)	Computational time
[28]	<i>K</i> -star algorithm	89.16	0.01 s
[29]	CNN	90.00	—
[30]	Random forest	90.54	—
[31]	Long short-term memory network (LSTM)	94.00	—
[29]	ResNet	90.00	—
[21]	Statistical analysis and regression algorithm	91.25	—
[32]	ResNet 50	93.80	90 s
[20]	J48 decision tree	94.58	—
[24]	Random committee classifier	90.41	—
Proposed	WiSARD	97.92	0.008 s

“—” indicates that the computational time data were not available.

computational time of 0.008 s. From the observations listed in Table 21, one can infer that various machine learning algorithms like *k* star, random forest, J48, and random committee displayed good classification accuracies with values of 89.16%, 90.54%, 94.58%, and 90.41%, respectively. It can be observed that the J48 algorithm achieved the highest classification accuracy among the machine learning algorithms. On the other hand, deep learning algorithms displayed even an enhanced classification with CNN (90.00%), LSTM (94.00%), ResNet (90.00%), and ResNet 50 (93.80%) models. However, the computational time of machine learning algorithms was found to be low in comparison to deep learning models from the literature observations made.

## 5. Conclusion

In this investigation, a weightless neural network (WNN) is applied to monitor the condition of vehicle tires. The study specifically employs the WiSARD classifier, a variant of WNN, to assess the efficacy of this classification methodology. The research methodology encompasses the

extraction of statistical, histogram, and ARMA features from the dataset, followed by the selection of pertinent features using a J48 decision tree. Subsequently, the WiSARD classifier is used to classify these chosen features into one of the four tire conditions under examination. Furthermore, an exhaustive exploration of various hyperparameters is conducted to identify the optimal configuration for the WiSARD classifier, with the aim of achieving the highest possible level of accuracy. The outcomes derived from these experiments reveal that the combination of the WiSARD classifier with histogram features delivers an exceptional accuracy rate of 97.92% when operating with the optimal hyperparameter settings, as outlined in Table 20. Of particular note, these testing results are obtained within an incredibly brief computational time of just 0.008 seconds, underscoring the feasibility of implementing this method in real-time scenarios. This proposed approach has the potential to substantially enhance the precision and immediacy of tire condition detection and diagnosis, thereby fortifying the effectiveness and reliability of tire condition monitoring systems. Furthermore, this approach can be seamlessly integrated into real-time monitoring systems, ensuring the

provision of instantaneous results. Looking forward, there is an opportunity to focus on the development of on-board solutions that offer cost-effective benefits to end-users.

## Data Availability

The datasets generated or examined in the current study are accessible from the corresponding author upon reasonable request.

## Conflicts of Interest

The authors declare that they have no conflicts of interest that could have appeared to influence the work reported in this paper.

## Authors' Contributions

N.V.S., V.S.M., and S.V. conceptualized the study. N.V.S., S.V., and A.P.S. proposed the methodology. S.A. and N.V.S. provided software. S.A., N.V.S., and S.V. contributed to validation. A.P.S. performed formal analysis, contributed to visualization, and provided resources. A.P.S. and N.V.S. performed investigation. N.V.S. contributed to data curation. S.A. wrote the original draft. N.V.S., S.V., A.P.S., and V.S.M. reviewed and edited the article. S.V. performed supervision. V.S.M. and S.V. provided project administration. All authors have read and agreed to the published version of the manuscript.

## References

- [1] F. A. Abdulla, N. A. Jebur, and H. A. Jasim, "Effect of using the nitrogen in automotive tires on vibration and fuel consumption," *IOP Conference Series: Materials Science and Engineering*, vol. 870, no. 1, Article ID 012167, 2020.
- [2] A. B. Muturatnam, N. V. Sridharan, A. P. Sreelatha, and S. Vaithyanathan, "Enhanced tyre pressure monitoring system for nitrogen filled tyres using deep learning," *Machines*, vol. 11, no. 4, p. 434, 2023.
- [3] V. Mazur, "Experimental research in automobile non-pneumatic tire force heterogeneity," *MATEC Web of Conferences*, vol. 224, Article ID 02019, 2018.
- [4] A. A. Popov and Z. Geng, "Modelling of vibration damping in pneumatic tyres," *Vehicle System Dynamics*, vol. 43, no. sup1, pp. 145–155, 2005.
- [5] N. N. Hasan, A. Arif, M. Hassam, S. S. Ul Husnain, and U. Pervez, "Implementation of tire pressure monitoring system with wireless communication," in *Proceedings of the 2011 International Conference on Communications, Computing and Control Applications (CCCA)*, pp. 1–4, Hammamet, Tunisia, September 2011.
- [6] L. M. Silalahi, M. Alaydrus, A. D. Rochendi, and M. Muhtar, "Design of tire pressure monitoring system using A pressure sensor base," *Sinergi*, vol. 23, no. 1, p. 70, 2019.
- [7] D.-H. Lee, D.-S. Yoon, and G.-W. Kim, "New indirect tire pressure monitoring system enabled by adaptive extended kalman filtering of vehicle suspension systems," *Electronics*, vol. 10, no. 11, p. 1359, 2021.
- [8] C. Li, R.-V. Sánchez, G. Zurita, M. Cerrada, and D. Cabrera, "Fault diagnosis for rotating machinery using vibration measurement deep statistical feature learning," *Sensors*, vol. 16, no. 6, p. 895, 2016.
- [9] H. Shao, H. Jiang, X. Zhang, and M. Niu, "Rolling bearing fault diagnosis using an optimization deep belief network," *Measurement Science and Technology*, vol. 26, no. 11, Article ID 115002, 2015.
- [10] Z. Chen, C. Li, and R. V. Sánchez, "Multi-layer neural network with deep belief network for gearbox fault diagnosis," *Journal of Vibroengineering*, vol. 17, 2015.
- [11] Z. Ullah, B. A. Lodhi, and J. Hur, "Detection and identification of demagnetization and bearing faults in PMSM using transfer learning-based VGG," *Energies*, vol. 13, no. 15, p. 3834, 2020.
- [12] S. Manikandan and K. Duraivelu, "Fault diagnosis of various rotating equipment using machine learning approaches a review," *Proceedings of the Institution of Mechanical Engineers Part E: Journal of Process Mechanical Engineering*, vol. 235, no. 2, pp. 629–642, 2021.
- [13] S. Shahrabadi, Y. Castilla, M. Guevara, L. G. Magalhães, D. Gonzalez, and T. Adão, "Defect detection in the textile industry using image-based machine learning methods: a brief review," *J Phys Conf Ser*, vol. 2224, no. 1, Article ID 012010, 2022.
- [14] T. B. Luderemir, "Weightless neural models: an overview," *Women in Computational Intelligence*, pp. 335–349, 2022.
- [15] L. Santiago de Araújo, V. C. Patil, C. B. Prado et al., "Design of robust, high-entropy strong PUFs via weightless neural network," *Journal of Hardware and Systems Security*, vol. 3, pp. 235–249, 2019.
- [16] Z. Susskind, A. Arora, I. D. S. Miranda et al., "Weightless neural networks for efficient edge inference," in *Proceedings of the International Conference on Parallel Architectures and Compilation Techniques*, pp. 279–290, New York, NY, USA, December 2022.
- [17] N. V. Sridharan, J. V. Joseph, S. Vaithyanathan, and M. Aghaei, "Weightless neural network-based detection and diagnosis of visual faults in photovoltaic modules," *Energies*, vol. 16, no. 15, p. 5824, 2023.
- [18] M. De Gregorio and M. Giordano, "The WiSARD classifier," 2016, <https://www.esann.org/sites/default/files/proceedings/legacy/es2016-63.pdf>.
- [19] M. De Gregorio and M. Giordano, "An experimental evaluation of weightless neural networks for multi-class classification," *Applied Soft Computing*, vol. 72, pp. 338–354, 2018.
- [20] P. S. Anoop and V. Sugumaran, "Effect of wheel balancing on tyre condition monitoring system using vibration signals through statistical features and machine learning techniques," *Journal of Intelligent and Fuzzy Systems*, vol. 43, no. 1, pp. 561–573, 2022.
- [21] P. S. Anoop and V. Sugumaran, "Comparative study on different balancing conditions of an air filled tyre using statistical features and classification via regression algorithm," *IOP Conference Series: Materials Science and Engineering*, vol. 1012, no. 1, Article ID 012031, 2021.
- [22] P. S. Anoop and V. Sugumaran, "Classifying machine learning features extracted from vibration signal with logistic model tree to monitor automobile tyre pressure," *SDHM Structural Durability and Health Monitoring*, vol. 11, 2017.
- [23] A. Joshua and V. Sugumaran, "Crack detection and localization on wind turbine blade using machine learning algorithms: a data mining approach," *Structural Durability & Health Monitoring*, vol. 13, no. 2, pp. 181–203, 2019.
- [24] P. S. Anoop, P. Nair, and V. Sugumaran, "Influence of unbalance on classification accuracy of tyre pressure monitoring

- system using vibration signals,” *Structural Durability & Health Monitoring*, vol. 15, no. 3, pp. 261–279, 2021.
- [25] M. Staffa, M. Giordano, and F. Ficuciello, “A WiSARD network approach for a BCI-based robotic prosthetic control,” *International Journal of Social Robotics*, vol. 12, no. 3, pp. 749–764, 2020.
- [26] A. Rattan, N. Venkatesh S, V. Sugumaran, and P. S. Anoop, “Monitoring the condition of nitrogen-filled tires using weightless neural networks,” *Automatika*, vol. 65, no. 2, pp. 523–537, 2024.
- [27] H. Haghghat, M. Mirzarezaee, B. N. Araabi, and A. Khadem, “A sex-dependent computer-aided diagnosis system for autism spectrum disorder using connectivity of resting-state fMRI,” *Journal of Neural Engineering*, vol. 19, no. 5, Article ID 056034, 2022.
- [28] P. S. Anoop, “Implementing K-star algorithm to monitor tyre pressure using extracted statistical features from vertical wheel hub vibrations,” *Indian Journal of Science and Technology*, vol. 9, pp. 1–7, 2016.
- [29] Z. Ziaukas, A. Busch, M. Wielitzka, T. Ortmaier, and J.-P. Kobler, “Classification of tire pressure in a semitrailer using a convolutional neural network,” in *Proceedings of the 2020 IEEE International Conference on Mechatronics and Automation (ICMA)*, pp. 181–185, Beijing, China, March 2020.
- [30] O. Svensson, S. Thelin, S. Byttner, and Y. Fan, “Indirect tire monitoring system machine learning approach,” *IOP Conference Series: Materials Science and Engineering*, vol. 252, Article ID 012018, 2017.
- [31] X. Wang, Z. Chen, W. Cao et al., “Artificial neural network-based method for identifying under-inflated tire in indirect TPMS,” *IEEE Access*, vol. 8, pp. 213799–213805, 2020.
- [32] V. Vasan, N. V. Sridharan, A. Prabhakaranpillai Sreelatha, and S. Vaithyanathan, “Tire condition monitoring using transfer learning-based deep neural network approach,” *Sensors*, vol. 23, no. 4, p. 2177, 2023.